# Correction to "Inverse analysis of the role of soil vertical heterogeneity in controlling surface soil state and energy partition"

Kun Yang, Toshio Koike, Baisheng Ye, and Luis Bastidas

Received 22 April 2005; published 1 July 2005.

**Citation:** Yang, K., T. Koike, B. Ye, and L. Bastidas (2005), Correction to ''Inverse analysis of the role of soil vertical heterogeneity in controlling surface soil state and energy partition,'' *J. Geophys. Res.*, *110*, D13105, doi:10.1029/2005JD006114.

[1] In the paper "Inverse analysis of the role of soil vertical heterogeneity in controlling surface soil state and energy partition" (*Journal of Geophysical Research*, *110*, D08101, doi:10.1029/2004JD005500, 2005), equations (20), (22), and (23) were incorrect. The corrected equations appear below.

$$\overline{K_s}(sand) = 7.0556 \times 10^{-6.884+0.0153sand}\ \mathrm{m\ s^{-1}}, \tag{20}$$

$$\overline{\Psi_s}(sand) = -0.01 \times 10^{1.88-0.0131sand}\ \mathrm{m}, \tag{22}$$

$$\overline{b}(clay) = 2.91 + 0.159clay. \tag{23}$$


0148-0227/05/2005JD006114$09.00

# Inverse analysis of the role of soil vertical heterogeneity in controlling surface soil state and energy partition

Kun Yang and Toshio Koike
Department of Civil Engineering, University of Tokyo, Tokyo, Japan

Baisheng Ye
Cold and Arid Regions Environmental and Engineering Research Institute, Chinese Academy of Sciences, Gansu, China

Luis Bastidas
Department of Civil and Environmental Engineering and Utah Water Research Laboratory, Utah State University, Logan, Utah, USA

Received 8 October 2004; revised 19 January 2005; accepted 10 February 2005; published 20 April 2005.

[1] Surface soil moisture and temperature have been widely addressed in land surface processes modeling and satellite remote sensing because they play a key role in land surface energy and water budget. However, it is rather difficult for some land surface models to reproduce the surface soil state in areas with high soil vertical heterogeneity because these models use a single parameter set to characterize soil hydraulic and thermal processes. This study develops a single-source land surface model to parameterize this heterogeneity. Its soil parameters are inversely estimated by minimizing a cost function that is objectively determined by the discrepancy between observed and model-predicted values of soil moisture and temperature. The approach is then used to investigate how the soil vertical heterogeneity affects subsurface processes and thus controls soil surface state and surface energy budget. This approach is applied to a synthetic numerical experiment and a Tibet field experiment, where the horizontal heterogeneity can be neglected. We indicate that (1) vertical heterogeneous soils cannot be effectively approximated by vertically homogenous soils in a land surface model no matter how the soil parameters are adjusted; (2) soil vertical heterogeneity obviously affects soil subsurface processes and plays a very important role in controlling surface soil wetness and surface energy partition; and (3) in particular, the existence of dense vegetation roots in topsoils may significantly reduce thermal conductivity, increase soil water potential, and enhance surface evaporation. We therefore conclude that it is indispensable to take the soil vertical heterogeneity into account in land surface models, although some of them still assume vertically uniform soil parameters.

**Citation:** Yang, K., T. Koike, B. Ye, and L. Bastidas (2005), Inverse analysis of the role of soil vertical heterogeneity in controlling surface soil state and energy partition, *J. Geophys. Res.*, *110*, D08101, doi:10.1029/2004JD005500.

## 1. Introduction

[2] Understanding land-atmosphere interactions may improve the predictability of precipitation on seasonal timescales in some regions [*Koster et al.*, 2004]. Much attention has been paid to the prediction of surface soil moisture and temperature because they play a key role in controlling surface energy partition. Experiences of the Global Soil Wetness Project (GSWP) [*Dirmeyer et al.*, 1999] and Project for the Intercomparison of Land Surface Parameterization Schemes (PILPS) [*Pitman and Henderson-Sellers*, 1998] indicate that the prediction of surface soil state (particularly soil wetness) is quite model-dependent, because of a number of problems such as model structure, parameter specification, and so on. In this study, we intend to evaluate the effects of soil vertical heterogeneity in land surface processes, which can play an important role in some regions but have not been widely addressed in land surface models (LSMs). An early study [*Dirmeyer and Zeng*, 1999] shows soil vertical heterogeneity may affect evaporation and runoff, but the long-term effects are small. Their study is simple and only considers vertical heterogeneity of soil porosity. This study will investigate this issue comprehensively.

[3] Soil structures are not only horizontally heterogeneous but also often vertically heterogeneous. The top layer of a soil can have different soil textures and amounts of organic matters from the deep layer. A typical example is the prairie in the Central and Eastern Tibetan Plateau, where the surface is covered by short vegetation. The vegetation develops very plentiful roots in the top 10 to 20 centimeters


0148-0227/05/2004JD005500$09.00

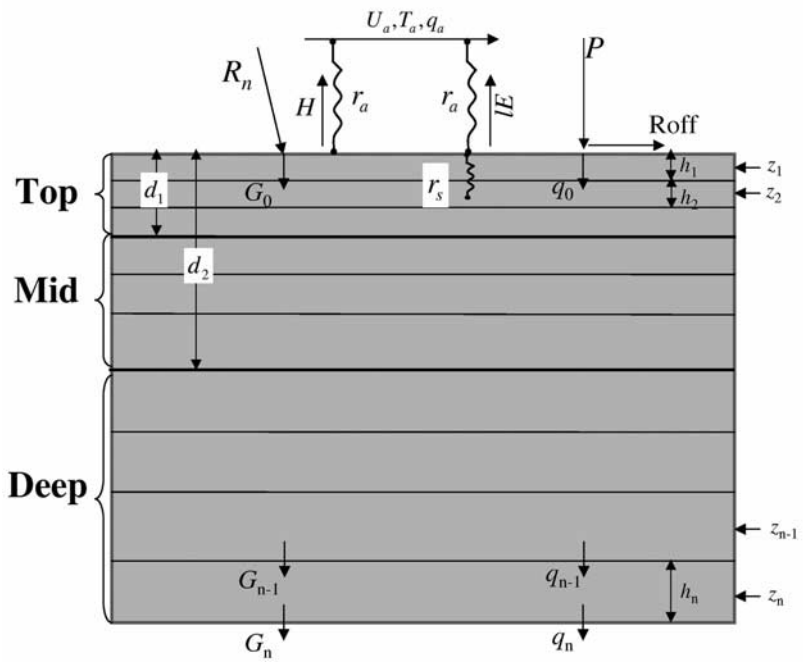


**Figure 1.** Schematic of the single-source land surface model used in this study. There are three soil domains (Top, Mid, Deep), each of which contains multiple computational layers. All the symbols have their common meanings.

to adapt the harsh climate in the plateau. The roots share a quite large amount of volume of the topsoil and may change soil properties. For example, the soil porosity in the topsoil can be as high as 0.6, much higher than in the deep soil, and the bulk density can be as low as 800 kg $m^{-3}$, much lower than in the deep soil. Numerical experiments [*Koudelova*, 2003; *Gao et al.*, 2004] have shown the Simple Biosphere model (SiB2) [*Sellers et al.*, 1996] cannot produce observed soil moisture, ground temperature, and surface energy partition at several plateau sites. These studies preliminarily suggest the limitations of current LSMs for vertically heterogeneous soils. A major reason for the poor performance is that these LSMs use a single parameter set to characterize soil properties and thus more or less wrongly parameterize subsurface processes in the vertically heterogeneous soils.

[4] To address the role of this heterogeneity in land surface processes, this study develops a LSM that can take soil vertical heterogeneity into consideration. Because some parameters are highly variable [*Abbaspour et al.*, 1999; *Eching et al.*, 1994] or are sensitive to change in the input-state-output response [*Pitman*, 1994], we use an inverse approach to estimate some soil parameters in this LSM, so that the model can reproduce the observed soil state. There are a number of inverse studies on soil hydraulic parameters [e.g., *Dane and Hruska*, 1983; *Kool and Parker*, 1988; *Toorman et al.*, 1992; *Eching et al.*, 1994; *Parkin et al.*, 1995; *Abbaspour et al.*, 1999] while fewer studies on soil thermal parameters [*Nir et al.*, 1992; *Hopmans et al.*, 2002]. Most of these early studies are applied to numerical or laboratory experiments, and focus on the estimate of either soil hydraulic properties or thermal properties from small samples. However, parameter estimation for patch-scale or regional-scale is indispensable for applications of LSMs and hydrological models. In this aspect, both manual calibrations [e.g., *Sellers et al.*, 1989; *Liang et al.*, 1994] and automatic calibration techniques [e.g., *Yapo et al.*, 1996; *Franks and Beven*, 1997] have been used. With the advent of new optimization algorithms [*Yapo et al.*, 1998], a multicriteria parameter estimation was developed by *Gupta et al.* [1998], which has already been applied to LSM calibrations, both offline [*Gupta et al.*, 1999; *Bastidas et al.*, 1999, 2003; *Leplastrier et al.*, 2002] and coupled to atmospheric models [*Liu et al.*, 2003, 2005].

[5] Traditionally, for performing a multiobjective optimization, it is crucial to prescribe a weight to each objective/measure in the overall cost function so that a trade-off between different measures can be reached. The type of the measures and the model errors are essential information for determining the weights. Many early studies [e.g., *Mishra and Parker*, 1989] subjectively estimate the weights for the measures without considering model errors. *Abbaspour et al.* [1999] proposed a new multiplicative formulation of the cost function, which does not require weight for different measures, but a single measure with the smallest errors might dominate the cost function. The multicriteria parameter estimation of *Gupta et al.* [1998] discards the classical paradigm for model calibration and does not need weight numbers. This method gives many preferred parameter sets (the so-called Pareto set) and can be used to evaluate model uncertainties and sensitivities; however, for a model application, one parameter set has to be selected from the Pareto set on the basis of a subjective criterion [*Sen et al.*, 2001]. In this study, we intend to propose a new objectively determined cost function for a multiobjective parameter estimation.

[6] In addition, this study uses detailed measurements of soil moisture and temperature at several soil depths to estimate soil parameters and investigate soil vertical heterogeneity, while many early studies only use near-surface soil moisture and ground temperature.

[7] The paper is organized as follows: first, we present the inverse approach. It consists of three main steps, composed of (1) a land surface model to predict soil moisture and temperature profiles and surface fluxes (section 2), (2) a cost function to express the discrepancy between observed and model-predicted values of soil moisture and temperature (section 3), and (3) an efficient scheme to search the global minimum of the cost function (section 4). Then, the inverse approach is used to investigate the effect of soil vertical heterogeneity on soil wetness, ground temperature, and surface energy partition (section 5). Finally, we summarize the results (section 6).

## 2. A Single-Source Land Surface Model

[8] The scope of this study is to address soil parameter estimation and the role of vertical heterogeneity. For this purpose, a simple single-source LSM would be more favorable than a dual-source LSM that parameterizes heat transfer in vegetation canopy. A single-source model does not distinguish the separate contribution to the turbulent fluxes from the vegetation and from the ground, and it usually has fewer parameters to be calibrated than a dual-source model. *Yang et al.* [2004] indicate that a single-source model is applicable to bare soil surfaces or sparsely and shortly vegetated surfaces.

[9] The single-source model used in this study is a simplified form of the dual-source simple biosphere model: SiB2 [*Sellers et al.*, 1996]. The model structure is shown in Figure 1 and has three distinct features: (1) flux parameterizations for bare soils and/or shortly vegetated surfaces are improved on the basis of recent experiments in the Tibetan Plateau; (2) soil subsurface water and heat flows are simulated by a multilayer scheme; and (3) soil vertical heterogeneity is parameterized. The model consists of a bulk parameterization of the surface turbulent fluxes, Richards' Law to calculate the soil water flow, and thermal diffusion equation to calculate the soil heat flow. The vertically heterogeneous soil column is approximated by two uniform domains: a near-surface soil domain and a bottom soil domain, and a transitional domain between the two. To accurately simulate soil heat flow and water flow, each domain consists of a number of layers, thinner in the top domain ($\sim$1 cm) and thicker in the bottom domain ($\sim$10 cm). The number of computational layers is adjustable. In our case studies (section 5), there are 30 or 40 computational layers, and the total soil depth is 1.6 m. The LSM is integrated over 2 $\sim$ 3 months with a time step of several minutes. More details are presented in the case studies (section 5).

### 2.1. Surface Flux Parameterization

[10] According to the single-source concept, we parameterize surface turbulent fluxes as follows:

$$H = \rho c_p \frac{\Theta_g - \Theta_a}{r_a}, \tag{1}$$

$$E = \rho \frac{q_s(T_g) rh_g - q_a}{r_a + r_{soil}}, \tag{2}$$

where $H$ (W m$^{-2}$) is the sensible heat flux, $E$ (kg m$^{-2}$ s$^{-1}$) is the evaporative flux, $\rho$ (kg m$^{-3}$) is the air density and $c_p$ (J kg$^{-1}$ K$^{-1}$) is the air specific heat at constant pressure. $\Theta_g$ (K) is the ground potential temperature and $\Theta_a$ (K) is the air potential temperature at a reference level. $q_s$ ($T_g$) (kg kg$^{-1}$) is the saturated specific humidity at temperature $T_g$ (K), and $q_a$ (kg kg$^{-1}$) is the specific humidity at the reference level. $r_a$ (s m$^{-1}$) is the heat transfer resistance from the ground surface to the reference level and $r_{soil}$ (s m$^{-1}$) is the soil surface resistance for evaporation. $rh_g$ is the equilibrium relative humidity near the soil surface, and is calculated by [*Hanks*, 1992]

$$rh_g = \exp\left(\psi_g g / R_w T_g\right), \tag{3}$$

where $g = 9.81$ m s$^{-2}$, $R_w = 461.5$ J kg$^{-1}$ K$^{-1}$, and $\psi_g$ (m) is soil water potential near the surface.

[11] Calculating the aerodynamic resistance $r_a$ needs the aerodynamic roughness length $z_0$ and the thermal roughness length $z_T$. The value of $z_0$ may be estimated from wind profiles, and the value of $z_T$ in the single-source model is parameterized following *Yang et al.* [2002]:

$$z_T = h_T \exp\left(-10 u_*^{1/2} |T_*|^{1/4}\right), \tag{4}$$

where $h_T = 70\nu/u_*$, $u_*$ is the friction velocity, $T_* \equiv -H/\rho c_p u_*$. $\nu$(m$^2$ s$^{-1}$) is the air kinematic viscosity. $\nu = \nu_0 \left(\frac{p_0}{p}\right)\left(\frac{T}{T_0}\right)^{1.754}$, $\nu_0 = 1.328 \times 10^{-5}$ m$^2$ s$^{-1}$, $p_0 = 1.013 \times 10^5$ Pa, and $T_0 = 273.15$ K [*Kondo*, 1994].

[12] The roughness length $z_T$ in equation (4) is scaled by a turbulence-related length $h_T$ rather than the roughness length $z_0$. *Yang et al.* [2002] shows equation (4) can be applied to a wide range of the surface-air temperature difference.

[13] The soil resistance $r_{soil}$ is often parameterized by exponential formulas [*van de Grind and Owe*, 1994; *Kondo*, 1994, pp. 194–198]. We use the form of *Sellers et al.* [1996]:

$$r_{soil} = \exp\lfloor 8.206 - 4.255 w_g \rfloor, \tag{5}$$

where $w_g = \theta_g/\theta_s$ is near-surface soil wetness. $\theta_g$ (m$^3$ m$^{-3}$) is near-surface soil water content, and $\theta_s$ (m$^3$ m$^{-3}$) is the soil porosity.

### 2.2. Soil Water Flow

[14] Soil water flow follows Richards' Law:

$$\theta_s \frac{\partial w}{\partial t} = -\frac{\partial q}{\partial z}, \tag{6}$$

$$q = -K(w)\left[\frac{\partial \psi(w)}{\partial z} - 1\right], \tag{7}$$

where $t$ (s) is the time, $z$ (m) is the soil depth, $w = \theta/\theta_s$ is the soil wetness, $q$ (m s$^{-1}$) is the water flux (positive if downward), $K$ (m s$^{-1}$) is the soil hydraulic conductivity, $\psi$(m) is the water potential.

[15] The hydraulic functions $K(w)$ and $\psi(w)$ are described by *Clapp and Hornberger* [1978]:

$$K(w) = K_s w^{2b+3}, \tag{8}$$

$$\psi(w) = \psi_s w^{-b}, \tag{9}$$

where $K_s$ (m s$^{-1}$), $\psi_s$ (m), and $b$ are hydraulic parameters.

[16] To solve the water content, the unknown in equations (6) and (7) can be soil water content, water potential or water flux. This study selects the water flux as the unknown and uses a finite difference method to solve it. The lower boundary condition is the drainage of water out of the bottom of the soil column [see *Sellers et al.*, 1996, equation (37)]. The upper boundary condition is the surface infiltration rate, which is usually horizontally heterogeneous and needs careful parameterization [*Liang et al.*, 1994; *Koster and Milly*, 1997]. In this study, we mainly emphasize the vertical heterogeneity instead of horizontal heterogeneity, so the infiltration rate is estimated by the minimum of water supply and water demand [*Sellers et al.*, 1996] as a first approximation:

$$q_0 = \min(P - E/\rho_w, \theta_s(1-w)h_1/\Delta t), \tag{10}$$

where $q_0$ (m s$^{-1}$) is the soil infiltration rate. $E$ (kg m$^{-2}$ s$^{-1}$) is the surface evapotranspiration, $P$ (m s$^{-1}$) is the rainfall rate, and $\rho_w$ (kg m$^{-3}$) is the water density. $h_1$ (m) is the thickness of the first computational layer near the surface ($\sim$1 cm), $\Delta t$ (s) is the temporal resolution ($\sim$5 min.).

### 2.3. Soil Thermal Flow

[17] Soil temperature variation is governed by the thermal diffusion equation:

$$\frac{\partial \rho_s c_s(w) T_s}{\partial t} = \frac{\partial}{\partial z}\left(\lambda_s(w)\frac{\partial T}{\partial z}\right), \tag{11}$$

where $T_s$ (K) is the soil temperature, $\rho_s c_s(w)$ (J K$^{-1}$ m$^{-3}$) is the volumetric soil heat capacity, $\lambda_s(w)$ (W m$^{-1}$ K$^{-1}$) is the thermal conductivity.

[18] The soil heat capacity is calculated by

$$\rho_s c_s(w) = \rho_d c_d + \rho_w c_w \theta_s w, \tag{12}$$

$$\rho_w c_w = 4.195 \times 10^6 \text{ J m}^{-3} \text{ K}^{-1}, \tag{13}$$

$$\rho_d c_d = (0.076 + 0.748\rho_d/\rho_w) \times 10^6 \text{ Jm}^{-3} \text{ K}^{-1}, \tag{14}$$

where $\rho_d$ (kg m$^{-3}$) is the bulk density of a dry soil, $c_d$ (J kg$^{-1}$ K$^{-1}$) is the specific heat capacity of the dry soil, and $\rho_w$ (kg m$^{-3}$) is the water density.

[19] The thermal conductivity depends on soil types and soil moisture. The formula of *Johansen* [1975] is recommended by *Farouki* [1986] and *Peters-Lidard et al.* [1998] after comprehensive investigations. We combine this formula with a formula recommended by the *Global Soil Data Task* [2000] and give the following one:

$$\lambda_s(w) = \lambda_d + (\lambda_m - \lambda_d)\exp[k_T(1 - 1/w)], \tag{15}$$

$$\lambda_d = (0.135\rho_d + 64.7)/(2700 - 0.947\rho_d), \tag{16}$$

$$\lambda_m = 0.5^{\theta_s}\left(7.7^{q_c}2.0^{1-q_c}\right)^{1-\theta_s}, \tag{17}$$

where $\lambda_d$ (W m$^{-1}$ K$^{-1}$) and $\lambda_m$ (W m$^{-1}$ K$^{-1}$) are the minimum and maximum soil thermal conductivity, respectively. $k_T$ is a coefficient and has a value of 0.36. $q_c$ is the quartz content in dry soils.

[20] The soil temperature is solved from equation (11) using a finite difference method. The lower boundary condition uses an exponential profile of soil heat flux [*Bhumralkar*, 1975]: $G_n = G_{n-1}\exp(-h_n/d_a)$. Here, $G_n$ and $G_{n-1}$ are the soil heat fluxes at the deepest two levels, and $h_n$ is the soil thickness between the two levels (see Figure 1). $d_a$ is the $e$ folding depth of the annual temperature wave. The upper boundary condition is the surface heat flux $G_0$:

$$G_0 = R_n - H - lE, \tag{18}$$

where $R_n = (1 - \alpha_g)R_{sw} + \varepsilon_g(R_{lw} - \sigma T_{sfc}^4)$ is the incoming net radiation on the surface, $R_{sw}$(W m$^{-2}$) is the downward short-wave radiation, $R_{lw}$(W m$^{-2}$) is the downward long-wave radiation, $\alpha_g$ is the surface albedo to short-wave radiation. $\varepsilon_g$ is the surface emissivity, $\sigma = 5.67 \times 10^{-8}$ W m$^{-2}$ K$^{-4}$ is the Stefan-Boltzmann constant, $l$(J kg$^{-1}$) is the specific heat of vaporization.

### 2.4. Parameterizing Soil Vertical Heterogeneity

[21] The model approximates a vertically heterogeneous soil column by a sandwich-like structure: a uniform top domain, a transitional middle domain, and a uniform bottom domain, as shown in Figure 1. The transitional domain is bounded by depths $d_1$ and $d_2$. The top domain and the bottom domain are characterized by distinct soil parameters ($\theta_s$, $\rho_d$, $K_s$, $\psi_s$, $b$, $\lambda_m$). The soil properties for the transitional domain are interpolated from the ones for the top and the bottom domains. Considering nonlinearity of soil properties, we interpolate soil functions instead of soil parameters following an exponential variation in the transitional domain:

$$A(w) = A_1(w)^x A_2(w)^{1-x}, \tag{19}$$

where $A(w)$ denotes any hydraulic function ($K(w)$, $\psi(w)$) or thermal function ($\lambda(w)$, $\rho_s c_s(w)$). Subscripts 1 and 2 represent the top domain and the deep domain, respectively. $x = (d_2 - z)/(d_2 - d_1)$.

### 2.5. Algorithm of the LSM

[22] The algorithm is as follows: (1) given all the model parameters and soil temperature and moisture profiles at initial time $t_0$, (2) calculate heat flux and evaporative flux according to equations (1) and (2); (3) solve water flux and water content according to equations (6) and (7) using a finite difference method; (4) with known energy fluxes at the surface, calculate soil temperature profile with equation (11) using a finite difference method; (5) go to step 2 until termination.

## 3. Inverse Model

### 3.1. Input Data

[23] Input data of the inverse model include forcing data to drive the LSM, and soil moisture and temperature profiles for model calibration. The forcing data are routinely measured at an automatic weather station (AWS). Soil moisture and temperature are measured by a soil moisture and

**Table 1.** Optimized Parameters of the Land Surface Model

| Parameter | Symbol | Unit | Lower Bound | Upper Bound | σ | |
|---|---|---|---|---|---|---|
| | | | | | Top | Bottom |
| Soil porosity | $\theta_s$ | $m^3\ m^{-3}$ | $(1-\sigma)\overline{\theta_s}$ | $(1+\sigma)\overline{\theta_s}$ | 0.46 | 0.23 |
| Hydraulic parameters | $\psi_s$ | m | $\overline{\psi_s}^{(1+\sigma)}$ | $\overline{\psi_s}^{(1-\sigma)}$ | 0.38 | 0.19 |
| | $b$ | — | $(1-\sigma)\overline{b}$ | $(1+\sigma)\overline{b}$ | 0.5 | 0.2 |
| Thermal parameter | $\lambda_m$ | $W\ m^{-1}\ K^{-1}$ | $(1-\sigma)\overline{\lambda_m}$ | $(1+\sigma)\overline{\lambda_m}$ | 0.2 | 0.2 |
| Soil depths | $d_1$ | m | 0 | 0.3 | | |
| | $d_2$ | m | $d_1$ + 0.05 m | 1.6 | | |

temperature measuring system (SMTMS). The SMTMS consists of multiple temperature sensors (accuracy $\sim$ 0.1 K) and TDR (time domain reflectometry) moisture sensors (accuracy $\sim$ 0.03), and the sampling frequency can be 30 $\sim$ 60 min or finer. Additional details about the case studies are presented in sections 5.1.1 and 5.2.1.

### 3.2. Optimized Parameters

[24] As shown in section 2, there are many parameters in the LSM. Surface albedo $\alpha_g$ can be derived from measured downward and upward short-wave radiations, or estimated by empirical formulas [*Pleim and Xiu*, 1995]. Aerodynamic roughness length $z_0$ can be derived from wind profiles [*Kohsiek et al.*, 1993; *Yang et al.*, 2003]. The surface emissivity is specified as 0.97 since it does not significantly affect simulated results. The soil bulk density $\rho_d$ is measurable by experiments. The parameters $K_s$ and $\psi_s$ together determine soil water flow. They can be mutually dependent in inverse estimations, and thus it is difficult to simultaneously estimate both values. So we inversely estimate $\psi_s$ but roughly estimate $K_s$ by the following empirical formula [*Cosby et al.*, 1984]:

$$\overline{K_s}(sand) = 7.0556 \times 10^{-6.884+1.53sand}\ \mathrm{m\,s^{-1}}, \tag{20}$$

where *sand* denotes percentage of sand in dry soils.

[25] Therefore we select the parameters ($\theta_s$, $\psi_s$, $b$, $\lambda_m$, and $d_1$, $d_2$) in Table 1 for optimization.

[26] In addition, it is important to include prior information for effective soil parameter estimation [*Mertens et al.*, 2004]. We introduce several empirical formulas to estimate the soil hydraulic and thermal parameters [*Cosby et al.*, 1984; *Johansen*, 1975]:

$$\overline{\theta_s}(sand) = 0.489 - 0.00126sand, \tag{21}$$

$$\overline{\psi_s}(sand) = -0.01 \times 10^{1.88-1.31sand}\ \mathrm{m}, \tag{22}$$

$$\overline{b}(clay) = 2.91 + 15.9clay, \tag{23}$$

$$\overline{\lambda_m} = 0.5^{\theta_s}\left(7.7^{q_c}2.0^{1-q_c}\right)^{1-\theta_s}, \tag{24}$$

where $\overline{\theta_s}$, $\overline{\psi_s}$, $\overline{b}$, $\overline{\lambda_m}$ are roughly estimated parameter values of $\theta_s$, $\psi_s$, $b$, $\lambda_m$, respectively. *sand* and *clay* denote percentage of sand and clay in a dry soil, respectively, and quartz content $q_c$ in the dry soil is approximated by *sand*% if data is not available.

[27] Equations (21)–(24) are stochastic functions. Moreover, soil texture is often measured from soil samples, and their values contain some uncertainties due to soil heterogeneity. Therefore we introduce a coefficient σ to constrain the range of each optimized hydraulic/thermal parameter, as shown in Table 1. Its value for each parameter is determined with the consideration of the regression coefficient of equations (21)–(23) [*Cosby et al.*, 1984] and larger uncertainties in the top domain. Other parameters are bounded by two empirically determined numbers.

### 3.3. Objective Function

[28] The estimations of soil hydraulic parameters and thermal parameters cannot be separated because soil water flow and thermal flow are mutually dependent. In addition, a simultaneous estimation would yield smaller estimation errors for model parameters than sequential inversion of hydraulic properties followed by inversion for other properties, as suggested by *Mishra and Parker* [1989]. Therefore we simultaneously estimate soil hydraulic and thermal parameters. To establish a single-criterion for a multiobjective calibration, it is crucial to select weight numbers to maintain a trade-off between different measures in the cost function. The weights should be related to measurement and model errors of each variable. In general, a smaller weight is assigned to variables with larger errors, while a larger weight is assigned to variables with smaller errors. However, the weights in most of the early studies are subjectively estimated from measurements without considering measurement and model errors, although it has been recognized that the selection of weights can make significant differences to the estimated parameters. In this study, a two-step optimization procedure is proposed to minimize the following multiobjective function:

$$F = \frac{RMSE_T}{RMSE_{T,\min}} + \frac{RMSE_\theta}{RMSE_{\theta,\min}}, \tag{25}$$

where $RMSE_T$ and $RMSE_\theta$ represent the root mean square errors of soil temperature and soil water content over all measuring depths during the optimizing period, respectively. $RMSE_{T,\min}$ and $RMSE_{\theta,\min}$ are their minimum values.

[29] *Gupta et al.* [1999] also deem the errors of sensible heat fluxes and latent heat fluxes as measures in the multicriteria optimization. However, the flux data are often not available. For example, there were a number of sites measuring soil moisture and temperature but only two flux towers were available in the GAME-Tibet experiments. For wide applications, equation (25) only considers soil moisture and temperature for the optimization.

[30] Because in equation (25) the total measurement and model errors ($RMSE_T$ and $RMSE_\theta$) are scaled by their minimum values ($RMSE_{T,\min}$ and $RMSE_{\theta,\min}$), the dimensionless cost function takes into account measurement and

model errors. Distinct from early studies, the optimization includes two steps: step I, minimize $RMSE_T$ to obtain $RMSE_{T,\min}$, and minimize $RMSE_\theta$ to obtain $RMSE_{\theta,\min}$; step II, minimize the multiobjective function $F$ using the same data set and the same LSM as model operator.

## 4. Optimization Algorithm

[31] Optimizing parameters is a tough task in inverse problems of soil parameters because cost functions usually have multiparameters and are highly nonlinear, nonderivable and even discontinuous. The parameter space usually contains multiple minima. To find the global minimum, the Levenberg-Marquardt method [*Marquardt*, 1983] is widely used in inverse models [e.g., *Parkin et al.*, 1995; *Simunek and van Genuchten*, 1996; *Hopmans et al.*, 2002], but the inverse solution is sensitive to initial parameter guesses. To overcome this problem and to find globally optimal parameters, several effective methods has been developed in past twenty years, such as the simulated annealing [*Kirkpatrick et al.*, 1983], the annealing-simplex method [*Pan and Wu*, 1998], genetic algorithms [*Goldberg*, 1989], the sequential uncertainty fitting inverse [*Abbaspour et al.*, 1997]. This study adopts the Shuffled Complex Evolution method developed at The University of Arizona (SCE-UA) [*Duan et al.*, 1992, 1993]. This method is based on a synthesis of four concepts: (1) combination of deterministic and probabilistic approaches; (2) systematic evolution of a ''complex'' of points spanning the parameter space, in the direction of global improvement; (3) competitive evolution; and (4) complex shuffling. The synthesis of these elements makes the SCE-UA method effective and robust, and also flexible and efficient. It has been widely used in parameter calibration of various models.

## 5. Case Studies

[32] The inverse approach described above is used to calibrate the land surface model to two different data sets. The first is a numerically generated data set (hereafter identical twin). Numerically generated data sets are preferred over measured data sets because the ''true'' values of soil parameters are known and because ''measurement errors'' are controllable, resulting in less uncertainty in the analysis [*Toorman et al.*, 1992]. The second is a real data set collected at a GAME-Tibet (GEWEX Asian Monsoon Experiment in the Tibetan Plateau) site: Anduo. Inverse studies based on field data are more challenging since the inverse estimate will involve both large measurement errors and model errors. Both cases are used to clarify (1) how soil vertical heterogeneity can affect surface soil state and energy partition and (2) whether vertically heterogeneous soils can be approximated by uniform soils with adjustable parameters. In addition, we show the capacity of the inverse approach in estimating parameters by the identical twin study, and address effects of vegetation roots on soil properties by the Tibet case study.

### 5.1. Identical Twin

#### 5.1.1. Data Set

[33] The experiment design is very similar to that of the GAME-Tibet observations (see section 5.2.1). We assume that the total soil depth is 1.6 m and that this total depth is represented by three soil layers with thickness values of 0.10, 0.15, 1.35 meters (in other words, $d_1$ = 0.1 m, $d_2$ = 0.25 m). We also assume that the topsoil is a typical clay loam with a higher porosity and water potential and the bottom soil is a typical sandy loam with a lower porosity and water potential. The ground is a bare soil surface, and all horizontal heterogeneity is neglected. The surface is wetted by two-day continuous precipitation every 10 days in the first month, and dried in other days. The model is driven by diurnally varying wind speed, temperature, radiation, and a constant specific humidity.

[34] To examine the sensitivity of the inverse estimation, we deliberately introduce ''measurement'' errors and model errors. ''Measurements'' errors are introduced by using a coarse spatial resolution (30 layers) and temporal resolution (400 s) in the forward run, while using a relatively fine resolution (40 layers, 200 s) in the inverse estimation. Model errors are introduced by using different soil thermal and hydraulic functions in the forward run and the inverse runs. To describe the thermal conductivity, the inverse estimation sets $k_T = 0.36$ in equation (15), while the forward run assumes $k_T = 0.50$ in equation (15). To describe the hydraulic properties, the inverse estimation uses the four-parameter form ($\theta_s$, $b$, $K_s$, $\psi_s$) of equations (8) and (9) [*Clapp and Hornberger*, 1978], while the forward run uses a five-parameter form ($\theta_s$, $\theta_r$, $K_s$, $n$, $\alpha$) below [*van Genuchten*, 1980]:

$$K(w_e) = K_s w_e^{0.5}\left\{1 - \left[1 - w_e^{n/(n-1)}\right]^{(n-1)/n}\right\}^2, \qquad (26)$$

$$w_e = \left\{\frac{1}{1 + [100\alpha|\psi(w_e)|]^n}\right\}^{1-1/n}, \qquad (27)$$

where $w_e \equiv (\theta - \theta_r)/(\theta_s - \theta_r)$ is the effective saturation. $K_s$ (m s$^{-1}$), $n$, $\alpha$ (cm$^{-1}$), and $\theta_r$(m$^3$ m$^{-3}$) are hydraulic parameters. $\psi$ (m) is the soil water potential.

[35] The ''true'' values of soil parameters used in the forward run are shown in Table 2. Soil moisture is initialized by the residual values $\theta_r$, and soil temperatures are initialized with a constant temperature of 298 K. The model is then integrated 60 days (hereafter forward run). Soil moistures at five depths (0.04, 0.2, 0.6, 1.0, 1.6 m), and soil temperatures at nine depths (0.0, 0.04, 0.2, 0.4, 0.6, 0.8, 1.0, 1.3, 1.6 m) are recorded hourly, analogous to measurements at the GAME-Tibet experiments. These data are used as input data in the inverse estimation.

#### 5.1.2. Parameter Estimation and Optimized Output

[36] To address the importance of soil vertical heterogeneity, we carry out two calibrations: one considers the heterogeneity and uses different parameter sets to characterize top and bottom soils (hereafter heterogeneous case); the other ignores soil heterogeneity and uses a single uniform parameter set to characterize the heterogeneous soil (hereafter homogenous case). The model is initialized by interpolating ''true'' soil moisture and temperature to computational layers. A 5-day spin-up period is used to reduce the influence of the interpolation errors. For comparisons, results of the two cases are summarized in Figures 2–4. Figure 2 shows the estimated soil hydraulic

**Table 2.** Parameter Values of the Identical Twin Study in the Forward Run

| Parameter | Top Domain (Clay Loam) | Bottom Domain (Sandy Loam) |
|---|---|---|
| $\theta_s$, $m^3\ m^{-3}$ | 0.476 | 0.416 |
| $\rho_d$, $kg\ m^{-3}$ | 1309 | 1460 |
| $\theta_r$, $m^3\ m^{-3}$ | 0.141 | 0.043 |
| $K_s$, $m\ s^{-1}$ | $1.31 \times 10^{-6}$ | $7.11 \times 10^{-6}$ |
| $n$ | 1.35 | 1.41 |
| $\alpha$, $cm^{-1}$ | 0.00435 | 0.0230 |
| $\lambda_m$, $W\ m^{-1}\ K^{-1}$ | 1.59 | 2.16 |
| Soil depth, m | $0 \sim 0.1$ | $0.25 \sim 1.6$ |

and thermal properties; Figures 3 and 4 present the scatterplots showing the comparisons of simulated soil surface variable and energy partition between the ''truth'' run and the optimized run.

#### 5.1.2.1. Heterogeneous Case

[37] Figure 2 shows the comparison of soil hydraulic and thermal functions between the ''truth'' and the optimized one. They are calculated from the ''true'' parameters and optimized parameters ($\theta_s$, $\psi_s$, $b$, $\lambda_m$) for the topsoil domain and bottom soil domain. It shows that soil hydraulic functions in both domains and thermal properties in the top domain are well estimated by consideration of soil heterogeneity. The estimated thermal conductivity in the bottom domain shows larger errors than in the top domain, suggesting that it is more difficult to inversely estimate soil properties in the bottom domain. In general, surface soil state can have a significant variation in a short time while it takes a much longer time for deep-soil state to undergo an obvious change, so longer data records are a necessary condition for such an inversion of deep-soil parameters. In addition, the soil borders identified by the inversion ($d_1$ = 0.11 m, $d_2$ = 0.23 m) are comparable to the ''true'' values ($d_1$ = 0.10 m, $d_2$ = 0.25 m). Figure 3 presents a good agreement of ground temperature, near-surface (4 cm) soil water content, sensible heat fluxes, and latent heat fluxes between the optimized run and the ''truth'' run.

[38] In this identical twin study, we have introduced ''measurement'' errors in the input data by using a coarser resolution in the forward run and also model errors in the inversion by using different soil functions. It looks that these errors do not cause the inversion to become unstable. The soil parameters are reasonably estimated, although there are some minor differences between the ''true'' parameter values and the estimated values. The simulation using the estimated parameters almost reproduces the surface soil state and energy partition of the ''truth'' run, as shown Figure 3.

#### 5.1.2.2. Homogeneous Case

[39] Figure 2 also shows the estimated soil properties in the homogeneous case. It seems that the estimated values are close to that of the tops soil domain, perhaps because the estimated values are more dependent on the measurements in the topsoil than in the deep soil. The scatterplots in Figure 4 show that the surface state and energy partition of the optimized run severely deviate from the ''truth'' run. This can be explained as follows: in the experiment, the topsoil (clay loam) has a higher water potential than the deep soil, which restrains the water flow from the topsoil to deep soil. So the soil surface becomes wet and the ground temperature is relatively low. As a result, the sensible heat fluxes are small and the latent heat fluxes are large. In the homogenous case, only one parameter set is used to characterize the heterogeneous soil. Unavoidably, water flow from the top domain to the deep domain would be enhanced falsely, and a drier soil surface is erroneously simulated in this case. This would lead to high ground temperature and sensible heat fluxes, and low latent heat fluxes comparing to the ''truth'' run. Therefore this case suggests that an essentially heterogeneous soil cannot be

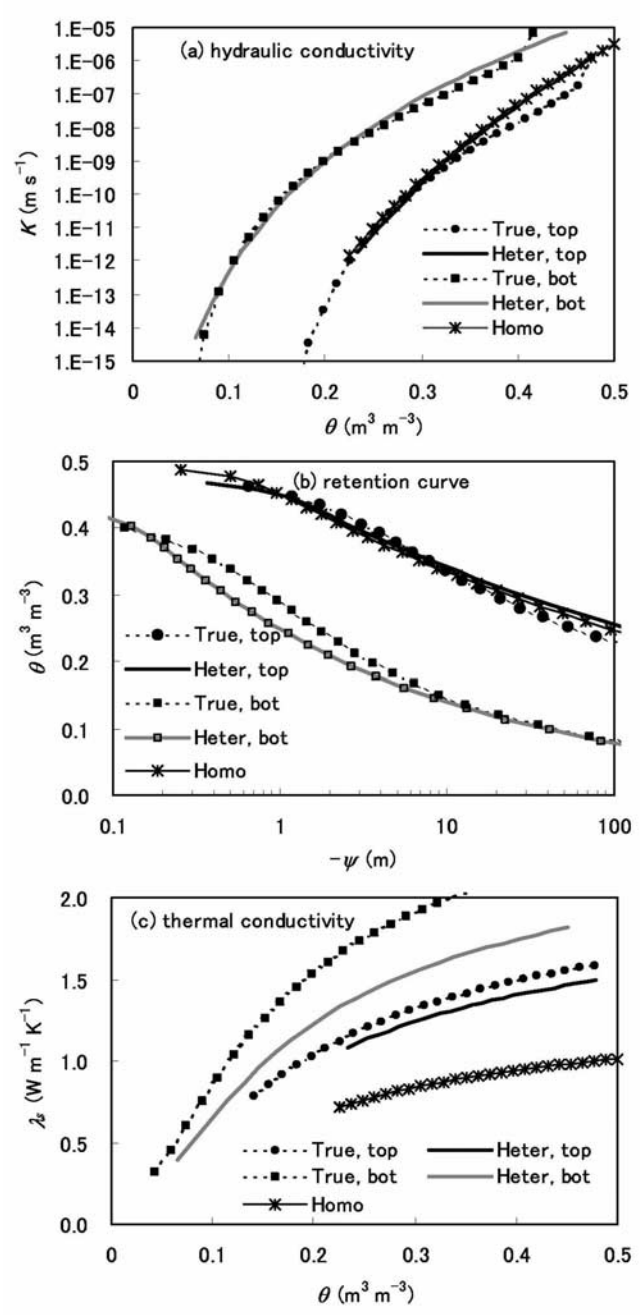


**Figure 2.** Comparison of soil hydraulic and thermal functions (for both the topsoil domain and the bottom soil domain) between the forward run and the optimized run of the identical twin study. Both the heterogeneous case (''Heter'') and homogeneous case (''Homo'') are shown.

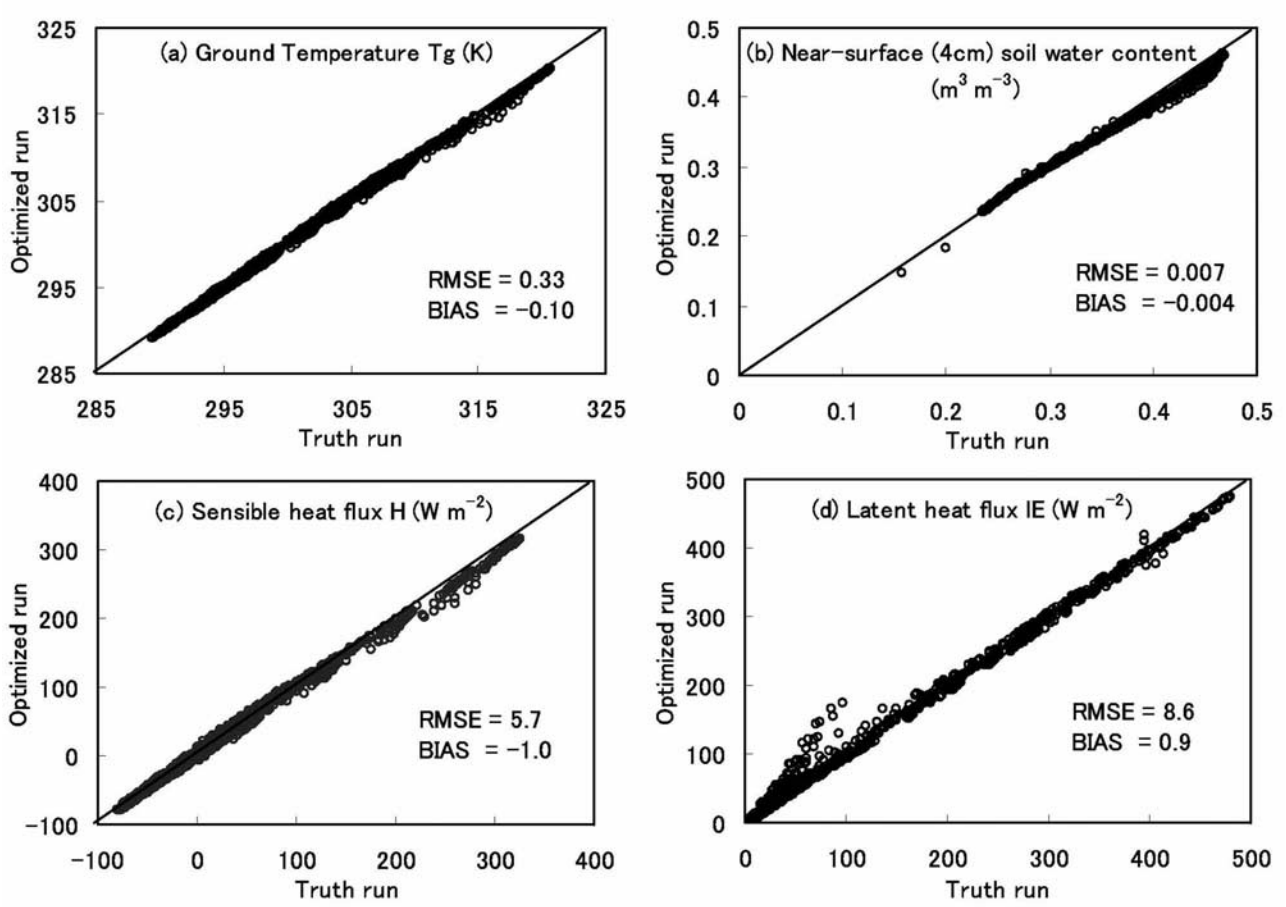


**Figure 3.** Comparison of ground temperature, near-surface soil moisture, sensible heat flux, and latent heat flux between the "true" values (from the forward run) and the optimized values (from the inverse calibration) for the heterogeneous case of the identical twin study. The root mean square error and bias are indicated for each variable.

approximated by a homogenous soil, no matter how the soil parameters are adjusted.

### 5.2. GAME-Tibet Anduo Site

#### 5.2.1. Description of Site and Data Set

[40] The GAME-Tibet Anduo site (Lat. 32.241°N, Lon. 91.635°E, Elev. 4700 m) locates at the central Tibetan Plateau. This site is covered by sparse and short grasses in the summer, but vegetation roots share a large volume of the surface soil layer in all seasons and the bulk density of the soil is therefore much lower than the deeper soil. This discontinuity of the soil structure is also found at other GAME-Tibet sites. Observations show soil water content is high near the surface, decreases in the transitional soil, and increases again in the deep soil. In some sensitivity studies of a dual-source land surface model, *Yang et al.* [2004] show that the vegetation can change the energy partition between the vegetation and the ground surface, but the energy partition between the sensible heat and the latent heat is insensitive to the leaf area index and the vegetation coverage for the plateau sparse and short prairie, and thus a single-source model is applicable to this site.

[41] To understand the land-atmosphere interactions on the plateau, intensive observations were carried out at Anduo during May–September 1998. Table 3 lists the field-collected data concerning the inverse estimation, including 30-minute-recorded forcing data for driving the LSM, hourly recorded soil temperature and moisture profiles for the inverse estimation. Moreover, there are two sets of observed energy partitions for verifying model output: in one set, the sensible heat fluxes were measured by the eddy-correlation technique, and the latent heat fluxes were derived from the surface energy budget equation (Note: the latent heat fluxes were actually measured by the eddy correlation, but the measurements are not trustable due to a sensor problem; see *Yang et al.* [2004] for more details); the other set was calculated from the observed air temperature and humidity profile by the Bowen ratio method.

[42] In addition, for comparison with inverse estimation, five soil samples (identified as 5A, 5B, 20A, 20B, and 60) were tested by laboratory experiments to analyze soil texture, porosity, bulk density (Table 4), and retention curve (Figure 5b).

#### 5.2.2. Parameter Estimation and Optimized Output

[43] A heterogeneous case that optimizes two parameter sets and a homogeneous case that optimizes one parameter set are applied to this study. The optimizing period should be long enough so that the soil moisture experiences a substantial variation from very dry to very wet, but its selection is often limited by available data length. At the

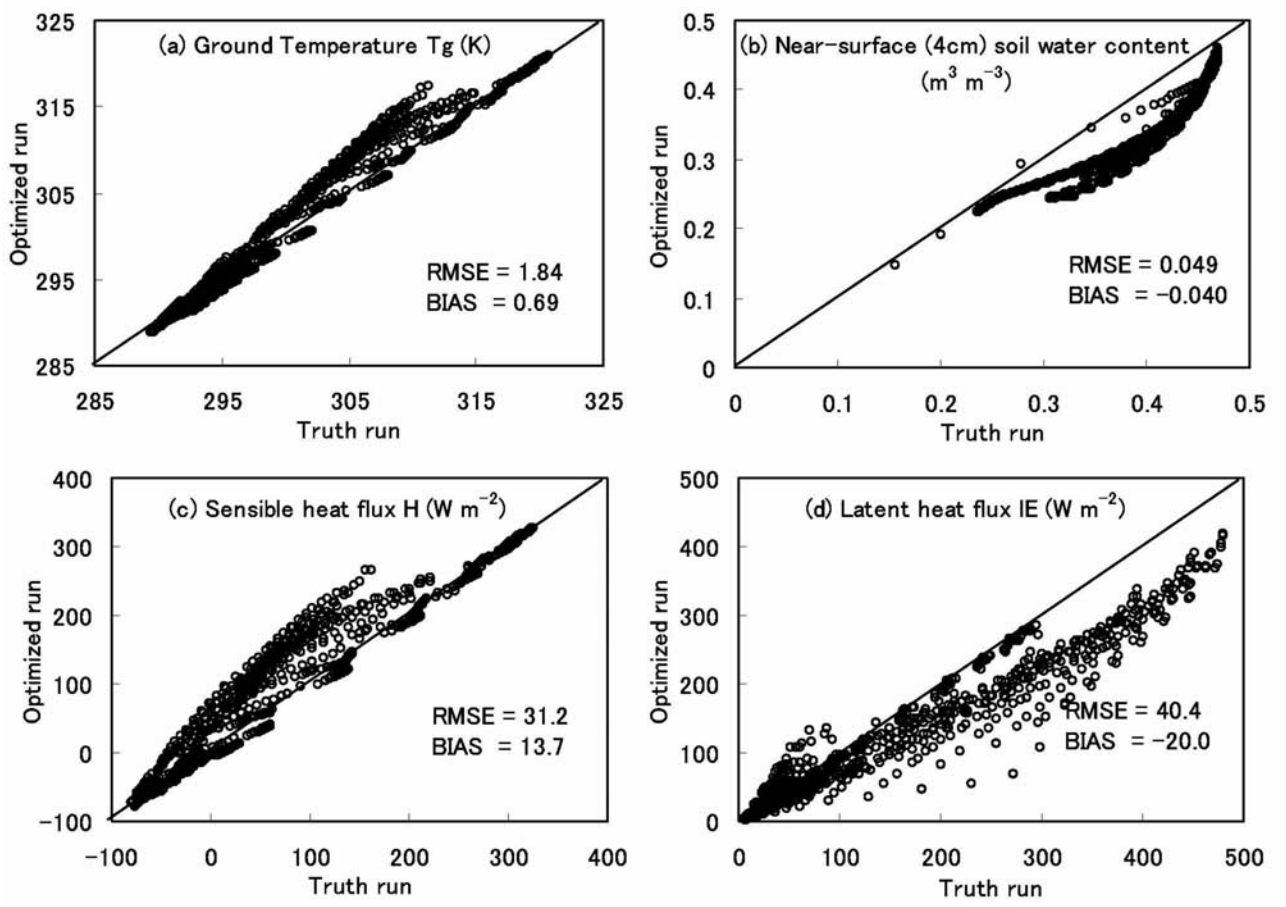


**Figure 4.** Same as Figure 3, except for the homogeneous case.

Anduo site, although five months (May–September) data are available, the soil experienced freezing and melting processes, which are not modeled in the LSM, in two months (May and September). Therefore a 75-day continuous data is used for the optimization, starting from 16 June 1998, when the soil was dry, to 30 August 1998, when the soil became wet. There are 40 computational soil layers, and the time step is 200 s. The model is initialized by interpolating measured soil moisture and temperature to computational layers, and a 5-day spin-up period is used to reduce the influence of the interpolation errors.

[44] The two cases use seasonally variable aerodynamic roughness length $z_0$ that was derived from wind profiles at this site [*Yang et al.*, 2003] since it is a key parameter of surface energy partition.

[45] For comparisons, the results are summarized in Table 5 and Figures 5–9. Table 5 shows the estimated soil properties, and Figure 5 shows the corresponding hydraulic and thermal functions. Figure 6 plots the root mean square error (RMSE) and mean biased error (BIAS) of soil temperature and moisture at measuring levels. Figure 7 shows a detailed depiction of the time serials behavior of ground temperature and of near-surface (4 cm) soil moisture. Figures 8 and 9 present the scatterplots showing the comparisons of energy partition between the simulation and the observation by eddy-correlation technique (or by Bowen ratio method).

#### 5.2.2.1. Parameter Evaluation

[46] This subsection briefly evaluates the estimated soil parameters for the heterogeneous case.

[47] 1. Soil vertical heterogeneity. The vertical heterogeneity is one major characteristic of the soil in the experimental area. Table 5 shows the optimized soil layer division occurs at the depth of 4.3 cm ($d_1$) and 21.9 cm ($d_2$) at Anduo site. In reality, it is difficult to discriminate between the top domain and the transitional domain from in situ observation because the grass roots pass through the top layer and

**Table 3.** Measurement Items and Levels at the GAME-Tibet Anduo Site, 1998

| Items | Height or Depth, m |
|---|---|
| *Planetary Boundary Layer (PBL) Station (30 Min. Average)* | |
| Wind speed and direction | 1.90, 6.00, 14.10 |
| Air temperature | 1.55, 5.65, 13.75 |
| Humidity | 1.55, 5.65, 13.75 |
| Pressure | surface |
| Precipitation | surface |
| Radiation | 14.0 |
| Turbulent fluxes | 2.85 |
| Soil temperature | 0.0, 0.05, 0.1, 0.2 |
| *SMTMS (60 Min. Average)* | |
| Soil moisture | 0.05, 0.2, 0.6, 1.0, 1.6, 2.58 |
| Soil temperature | 0.05, 0.2, 0.4, 0.6, 0.8, 1.0, 1.3, 1.6 |

**Table 4.** Soil Composition and Parameters Analyzed by Laboratory Experiments for the Anduo Site for Five Field Samples[a]

| Sample | Depth, cm | Sample Features | Composition, % | | | | $\rho_d$, kg m$^{-3}$ | $\theta_s$, m$^3$ m$^{-3}$ | $K_s$, $10^{-6}$ m s$^{-1}$ |
|---|---|---|---|---|---|---|---|---|---|
| | | | Gravel | Sand | silt | clay | | | |
| 5A | 5 | dense root | | N/A | | | 0.667 | 0.633 | <1.0 |
| 5B | 5 | dense root | 0.00 | 30.64 | 59.88 | 9.48 | 0.817 | 0.593 | 35.61 |
| 20A | 20 | little root, gravel | 3.69 | 69.02 | 19.83 | 7.46 | 1.378 | 0.440 | 48.83 |
| 20B | 20 | little root, gravel | 4.24 | 67.08 | 19.53 | 9.15 | 1.694 | 0.318 | 2.10 |
| 60 | 60 | little root, gravel | 3.35 | 76.56 | 10.12 | 9.97 | 1.426 | 0.370 | 27.73 |

[a]Two at 5 cm, two at 20 cm, and one at 60 cm.

extend to the transitional layer. Therefore the optimized boundary $d_1$ is meaningful only for the simulation of soil moisture and soil temperature. However, the deep boundary $d_2$ near 20 cm was roughly identified in the field experiments and features of the soil samples (see Table 4), which is close to the optimized depth.

[48] 2. Soil hydraulic properties. Figure 5b shows that both the experimental and optimized retention curves give a higher water potential for the topsoil than for the deep soil. The optimized retention curve for the deep soil is also agreeable with the experiment, but the curve for the top layer is different from the experiment. Possibly, the optimized parameters represent the mean properties of the soil domain, while the experimental parameters are deducted on the basis of small soil samples and thus their representativeness might be questionable if the soil layer is not uniform.

[49] 3. Soil thermal properties. The soil heat capacity can be estimated reliably because the soil porosity and soil moisture are reasonably reproduced and other quantities in equations (12)–(14) are measured directly. Unfortunately, there are no experimental data to directly verify the optimized soil thermal conductivity, but the small errors of the simulated soil temperatures at all depths (see Figure 6a)

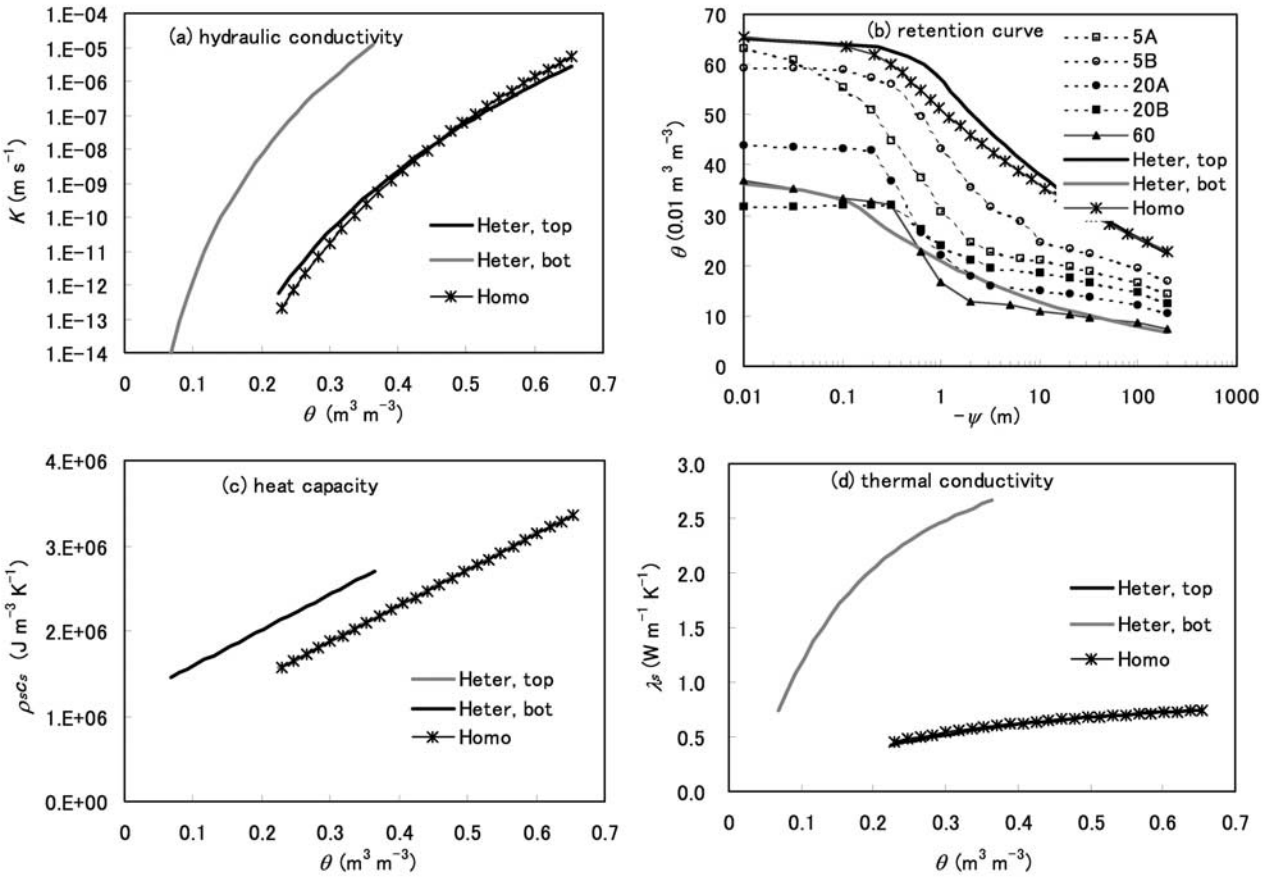


**Figure 5.** Comparison of soil hydraulic and thermal functions between two optimization cases (heterogeneous case and homogenous case) for the GAME-Tibet Anduo site, 1998. Retention curves analyzed from five soil samples (see Table 4) are also plotted in Figure 5b to compare with the optimized curves. Heter, heterogeneous case; Homo, homogeneous case; top, topsoil domain; bot, bottom soil domain. In Figures 5c and 5d, the curves for the ''Heter, bot'' and ''Homo'' fall on top of each other.

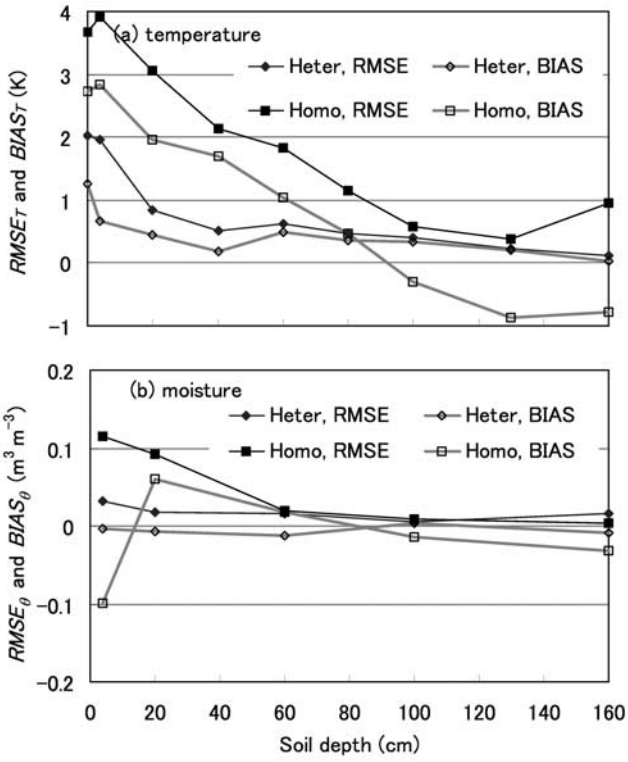


**Figure 6.** (a) Root mean square errors (RMSE) and biased errors (BIAS) of soil temperature at nine measuring depths and (b) soil moisture at five measuring levels for the heterogeneous case (''Heter'') and the homogeneous case (''Homo'') for the GAME-Tibet Anduo site during 16 June to 30 August 1998.

suggest that the optimized thermal parameters can give reasonable temperature simulations.

[50] The most impressive result (shown in Table 5 and Figure 5) is that the top domain and the deep domain have completely different properties, indicating that the existence of dense vegetation roots within the topsoil significantly changes its properties. Particularly, the topsoil has a high porosity, low thermal conductivity, and high soil water potential. The homogenous case produces the soil properties closer to the topsoil, similar to the identical twin case (see section 5.1.2.2).

#### 5.2.2.2. Model Output: Ground Temperature and Near-Surface Soil Wetness

[51] Figure 7 shows a detailed depiction of ground temperature (plot only for 15 July to 5 August to save space) and of near-surface (4 cm) soil moisture (for whole optimizing period) for the two cases. The near-surface soil moisture is reproduced by the heterogeneous case, but much underpredicted by the homogeneous case. As a result, the ground temperature of the heterogeneous case agrees well with the observed one, but the homogeneous case gives higher ground temperatures.

#### 5.2.2.3. Model Output: Surface Turbulent Heat Fluxes

[52] Figures 8 and 9 (parts a1 and b1) show the comparisons of energy partition between the simulation and the observation by the eddy-correlation technique, and parts a2 and b2 show the comparisons with the result of the Bowen ratio method. Again, we remind the reader that the ''observed'' latent heat fluxes in Figures 8–10 (part b1) were actually calculated from the surface energy budget equation based on eddy correlation-observed sensible heat fluxes and other observed energy fluxes, although the label of the horizontal axis is ''observed by eddy correlation.''

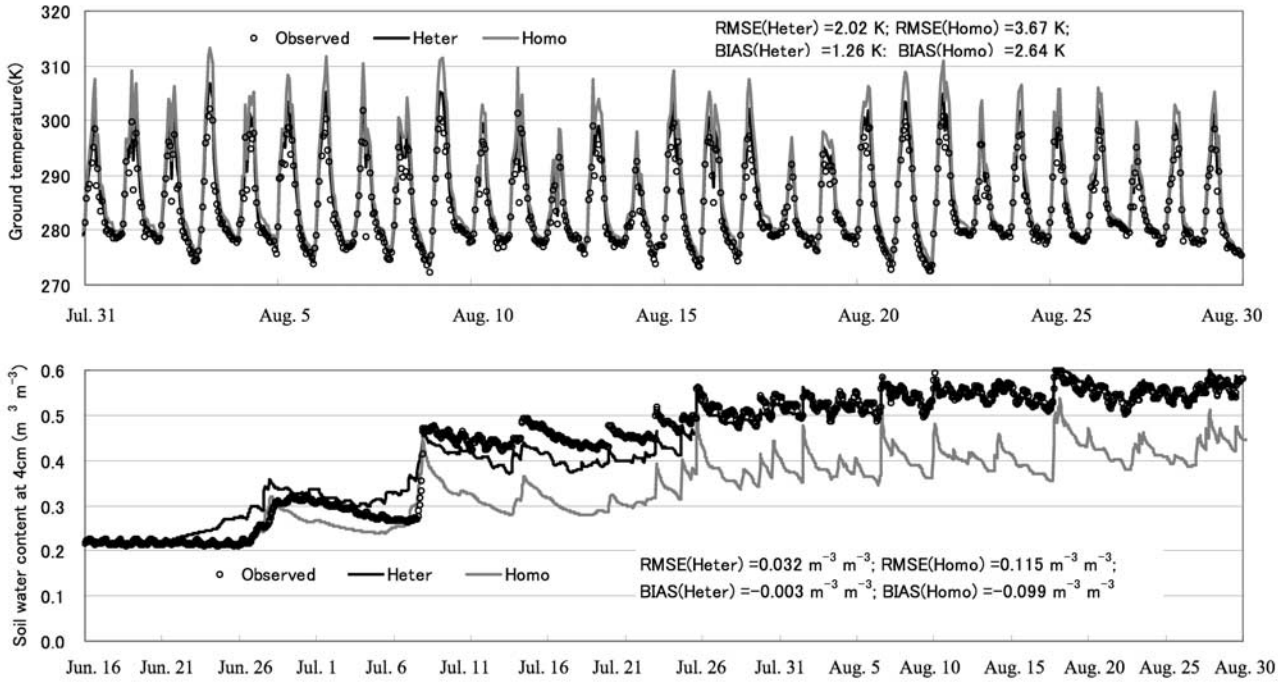


**Figure 7.** Comparison of ground temperature (plotted only for August to save space) and near-surface (4 cm) soil moisture (all the data are plotted) between the observations, the heterogeneous case (''Heter''), and the homogeneous case (''Homo'') for the GAME-Tibet Anduo site, 1998.

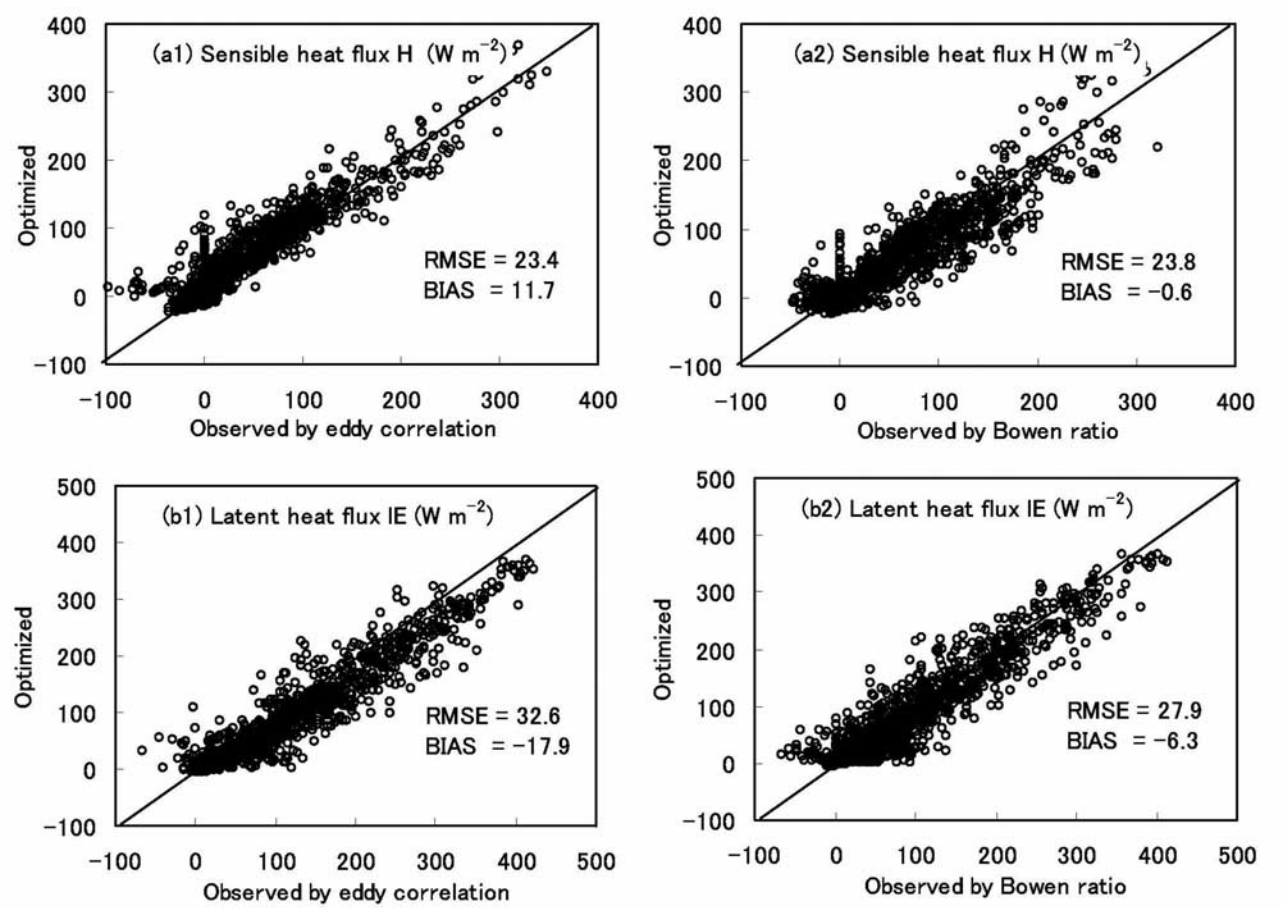


**Figure 8.** Comparison of sensible heat flux and latent heat flux between the observations and the optimized values (from the inverse calibration) for the heterogeneous case of the GAME-Tibet Anduo site during 16 June to 30 August 1998. The root mean square error and bias are indicated for each variable.

[53] For the heterogonous case (Figure 8), both the optimized sensible heat fluxes and latent heat fluxes are comparable to observations. Particularly, the optimized sensible heat fluxes ranges between the two sets of observations (by the eddy correlation and by the Bowen ratio), that is, a little larger than the observation by the eddy correlation while a little smaller than the observation by the Bowen ratio method. However, for the homogeneous case (Figure 9), it is clear that the sensible heat fluxes are overestimated while the latent heat fluxes are underestimated. Particularly, the simulated latent heat fluxes are much lower than that ''observed by eddy correlation.''

[54] We also have an additional run (hereafter experimental run) that uses the experimental parameters from soil samples of 5B (for the topsoil domain) and 20B (for the deep soil domain) and other optimized parameters in heterogeneous case. The experimental retention curves from the two soil samples (5B and 20B) are most close to the optimized one of the heterogeneous case (Figure 5b). This run gives smaller RMSE and BIAS of soil moisture and temperature than the homogenous case while obviously larger RMSE and BIAS than the heterogeneous case. Similarly, the energy partition prediction given by this run (Figure 10) is better than the homogenous case while worse than the heterogonous case. Therefore the optimized parameters in the heterogeneous case seem to be more representative than the experimental parameters in characterizing soil heat and water flows.

[55] These comparisons in surface energy budget suggest that the inverse approach considering soil vertical heterogeneity successfully provides a reasonable estimate of the turbulent fluxes, while fails to do so when the vertical heterogeneity is ignored or when the experimental parameters are used. The dense vegetation roots in the topsoil lead to high latent heat fluxes while low sensible heat fluxes. This, in turn, suggests the importance of soil vertical heterogeneity in controlling surface soil state and thus surface energy partition, and the vertically heterogeneous soil cannot be approximated by a homogenous soil in a land surface model.

[56] The above results are based on a 75-day (from 16 June to 30 August 1998) optimization. A 45-day (from 16 June to 30 July 1998) optimization gives similar results (not shown).

## 6. Conclusions

[57] This work develops an inverse system to evaluate the role of soil vertical heterogeneity in controlling surface soil wetness, ground temperature, and surface energy partition.

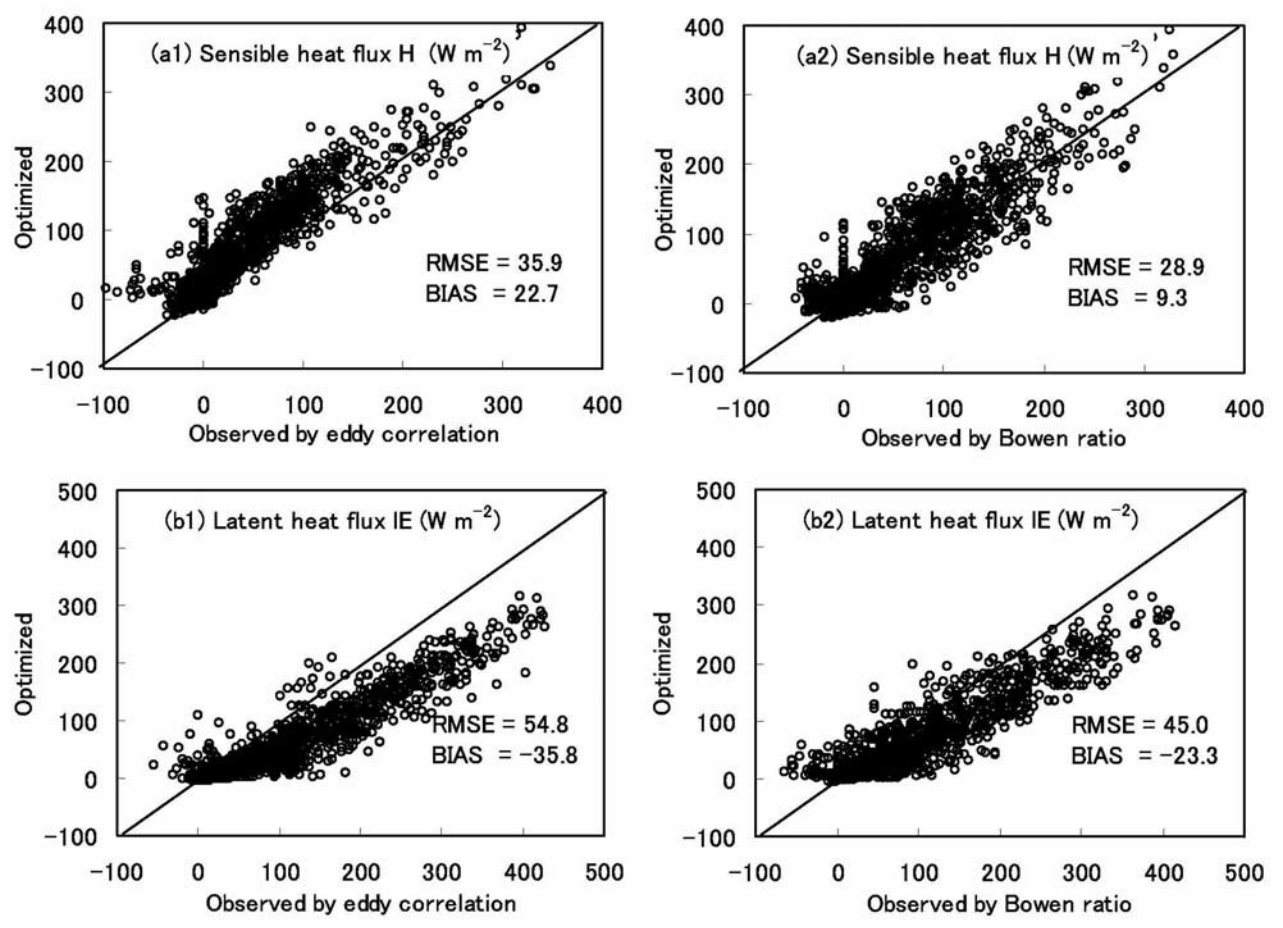


**Figure 9.** Same as Figure 8, except for the homogeneous case.

It consists of a single-source land surface model to predict soil moisture and temperature profiles and surface fluxes, a cost function to calculate the discrepancy between observed and model-predicted values of soil moisture and temperature, and an efficient scheme SCE-UA to search the global minimum of the cost function. We parameterize vertically heterogeneous soils by a sandwich-like model structure (two uniform domains and a transitional domain). We also present a dimensionless cost function that overcomes the difficulties in determining weight numbers while searching for a compromise solution in a multiobjective optimization. This inverse approach is able to approximately estimate soil thermal parameters and hydraulic parameters, particularly for the top domain. The estimated parameters might disagree with experimental results because the former represents the mean properties of a soil layer, while the latter only represents the properties of a small soil sample. As a result, the estimated parameters can more effectively characterize subsurface thermal and hydraulic processes.

[58] We apply this system to a numerical synthetic data set and a GAME-Tibet data set, where horizontal heterogeneity can be neglected. Both applications suggest that soil vertical heterogeneity plays a very important role in determining surface soil wetness, ground temperature, and thus surface energy partition. Particularly, dense vegetation roots in the Tibetan Plateau can significantly change the properties of the topsoil, such as high porosity, high soil water potential, and low thermal conductivity. The high soil water

**Table 5.** Estimated Soil Parameters of Two Optimization Cases for the Anduo Site Using the GAME-Tibet Data in 1998[a]

| | | Heterogeneous | | |
|---|---|---|---|---|
| Parameter | Symbol (Units) | Top Domain | Bottom Domain | Homogeneous |
| Soil depths | (cm) | 0 ∼ 4.3 | 21.9 ∼ 160 | — |
| Soil porosity | $\theta_s$ (m$^3$ m$^{-3}$) | 0.653 | 0.363 | 0.655 |
| Hydraulic parameters | $K_s$ ($10^{-6}$ m s$^{-1}$) | 2.71* | 11.2* | 5.51* |
| | $\psi_s$ (m) | −0.460 | −0.075 | −0.193 |
| | $b$ | 5.70 | 4.69 | 6.62 |
| Thermal parameter | $\lambda_m$ (W m$^{-1}$ K$^{-1}$) | 0.75 | 2.66 | 0.74 |

[a]The two optimization cases are the heterogeneous case and the homogeneous case. The values with asterisks are specified instead of optimized.

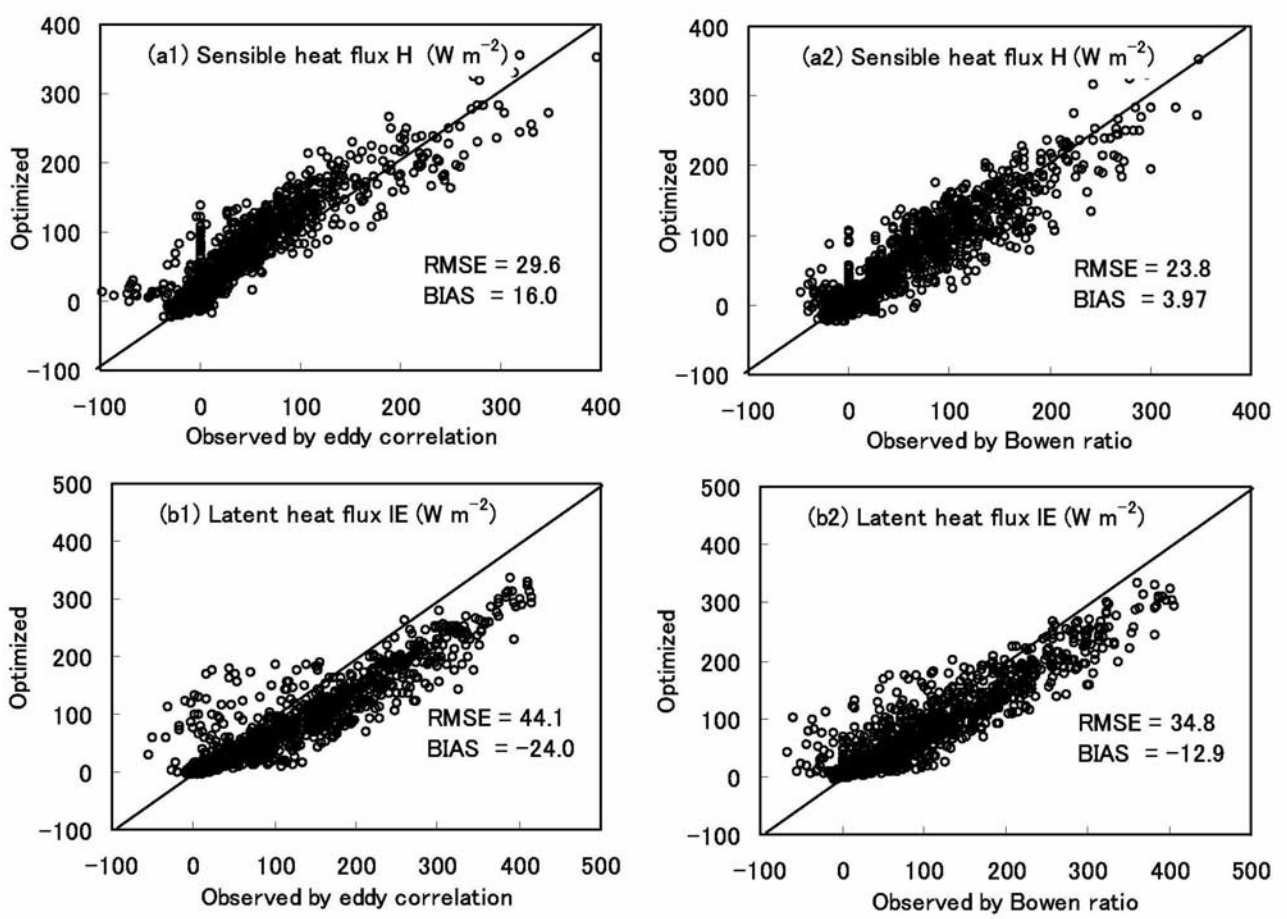


**Figure 10.** Same as Figure 8, except for the experimental run.

potential may result in a wet soil surface, and thus enhance evaporation fluxes while reduce ground temperature and sensible heat fluxes. Therefore the top domain, although shallow, is not only indispensable for sustaining the plateau ecological system, but also very important for controlling surface water and energy budget.

[59] Moreover, we indicate that the subsurface and surface processes in vertically heterogeneous soils cannot be parameterized in the framework of a single uniform soil. Therefore it seems to be difficult for some LSMs to account for the effects of the soil heterogeneity, since they use a single parameter set to characterize soil properties. Fortunately, the *Global Soil Data Task* [2000] is making efforts to build a globally covered data set of soil parameters, which can provide soil information of both horizontal heterogeneity and vertical heterogeneity. Although there are still many uncertainties inside the data set due to high variability of soil texture, it provides a possibility to update LSMs by considering soil vertical heterogeneity.

[60] **Acknowledgments.** The data at Anduo were collected through the GEWEX/GAME-Tibet project. The authors would like to acknowledge K. Ueno, Y. Ma, H. Ishikawa, K. Tanaka, and N. Hirose, who kindly provided in situ data and soil samples, and Paul Dirmeyer for his instructive suggestions.

## References

Abbaspour, K. C., M. T. van Genuchten, R. Schulin, and E. Schlappi (1997), A sequential uncertainty domain inverse procedure for estimating subsurface flow and transport parameters, *Water Resour. Res.*, *33*, 1879–1892.

Abbaspour, K. C., M. A. Sonnleitner, and R. Schulin (1999), Uncertainty in estimation of soil hydraulic parameters by inverse modeling: Example Lysimeter experiments, *Soil Sci. Soc. Am. J.*, *63*, 501–509.

Bastidas, L. A., H. V. Gupta, S. Sorooshian, W. J. Shuttleworth, and Z. L. Zhang (1999), Sensitivity analysis of a land surface scheme using multicriteria methods, *J. Geophys. Res.*, *104*(D16), 19,481–19,490.

Bastidas, L. A., H. V. Gupta, and S. Sorooshian (2003), Parameter, structure and performance evaluation for land surface models, in *Calibration of Watershed Models*, *Water Sci. and Appl. Ser.*, vol. 6, edited by Q. Duan et al., pp. 229–238, AGU, Washington, D. C.

Bhumralkar, C. M. (1975), Numerical experiments on the computation of ground surface temperature in an atmospheric general circulation model, *J. Appl. Meteorol.*, *14*, 1247–1258.

Clapp, R. B., and G. M. Hornberger (1978), Empirical equations for some hydraulic properties, *Water Resour. Res.*, *14*, 601–604.

Cosby, B. J., G. M. Hornberger, R. B. Clapp, and T. R. Ginn (1984), A statistical exploration of the relationships of soil moisture characteristics to the physical properties of soils, *Water Resour. Res.*, *20*, 682–690.

Dane, J. H., and S. Hruska (1983), In situ determination of soil hydraulic properties during drainage, *Soil Sci. Soc. Am. J.*, *47*, 619–624.

Dirmeyer, P. A., and F. J. Zeng (1999), Precipitation infiltration in the Simplified SiB land surface scheme, *J. Meteorol. Soc. Jpn.*, *77*, 291–303.

Dirmeyer, P. A., A. J. Dolman, and N. Sato (1999), The Global Soil Wetness Project: A pilot project for global land surface modeling and validation, *Bull. Am. Meteorol. Soc.*, *80*, 851–878.

Duan, Q., S. Sorooshian, and V. K. Gupta (1992), Effective and efficient global optimization for conceptual rainfall-runoff models, *Water Resour. Res.*, *28*, 1015–1031.

Duan, Q., V. K. Gupta, and S. Sorooshian (1993), A shuffled complex evolution approach for effective and efficient global minimization, *J. Optim. Theory Appl.*, *76*, 501–521.

Eching, S. O., J. W. Hopmans, and W. W. Wallender (1994), Estimation of in situ unsaturated soil hydraulic functions from scaled cumulative drainage data, *Water Resour. Res.*, *30*, 2387–2394.

Farouki, O. T. (1986), *Thermal Properties of Soils*, *Ser. Rock Soil Mech.*, vol. 11, 136 pp., Trans. Tech., Clausthal-Zellerfeld, Germany.

Franks, S. W., and K. J. Beven (1997), Bayesian estimation of uncertainty in land surface-atmosphere flux predictions, *J. Geophys. Res.*, *102*, 23,991–23,999.

Gao, Z., N. Chae, J. Kim, J. Hong, T. Choi, and H. Lee (2004), Modeling of surface energy partitioning, surface temperature, and soil wetness in the Tibetan prairie using the Simple Biosphere Model 2 (SiB2), *J. Geophys. Res.*, *109*, D06102, doi:10.1029/2003JD004089.

Global Soil Data Task (2000), Global Soil Data Products CD-ROM (IGBP-DIS) [CD-ROM], Int. Geosphere-Biosphere Programme, Data and Inf. Syst., Potsdam, Germany. (Available from Oak Ridge National Laboratory Distributed Active Archive Center, Oak Ridge, Tenn.; http://www.daac.ornl.gov)

Goldberg, D. E. (1989), *Genetic Algorithms in Search, Optimization, and Machine Learning*, 432 pp., Addison-Wesley, Boston, Mass.

Gupta, H. V., S. Sorooshian, and P. O. Yapo (1998), Toward improved calibration of hydrological models: Multiple and noncommensurable measures of information, *Water Resour. Res.*, *34*(4), 751–763.

Gupta, H. V., L. A. Bastidas, S. Sorooshian, W. J. Shuttleworth, and Z. L. Zhang (1999), Parameter estimation of a land surface scheme using multicriteria methods, *J. Geophys. Res.*, *104*(D16), 19,491–19,503.

Hanks, R. J. (1992), *Applied Soil Physics*, 2nd ed., 175 pp., Springer, New York.

Hopmans, J. W., J. Šimunek, and K. L. Bristow (2002), Indirect estimation of soil thermal properties and water flux using heat pulse probe measurements: Geometry and dispersion effects, *Water Resour. Res.*, *38*(1), 1006, doi:10.1029/2000WR000071.

Johansen, O. (1975), Thermal conductivity of soils, Ph.D. thesis, University of Trondheim, Trondheim, Norway. (*CRREL Draft Transl. 637*, Cold Reg. Res. and Eng. Lab., Hanover, N. H., 1977)

Kirkpatrick, S., C. D. Gelatt Jr., and M. P. Vecchi (1983), Optimization by simulated annealing, *Science*, *220*, 671–680.

Kohsiek, W., H. A. R. Bruin, H. The, and B. van Den Hurk (1993), Estimation of the sensible heat flux of a semi-arid area using surface radiative temperature measurements, *Boundary Layer Meteorol.*, *63*, 213–230.

Kondo, S. (1994), *Hydrometeorology: Water and Energy Budget on Ground Surfaces* (in Japanese), 348 pp., Asakura, Japan.

Kool, J. B., and J. C. Parker (1988), Analysis of the inverse problem for transient unsaturated flow, *Water Resour. Res.*, *24*, 817–830.

Koster, R. D., and P. C. D. Milly (1997), The interplay between transpiration and runoff formulations in land surface schemes used with atmospheric models, *J. Clim.*, *10*, 1578–1590.

Koster, R. D., P. A. Dirmeyer, Z. Guo, and GLACE Team (2004), Regions of strong coupling between soil moisture and precipitation, *Science*, *305*, 1138–1140.

Koudelova, P. (2003), Coupling a land surface scheme with a distributed hydrologic model and applying in the Tibetan Plateau, 143 pp., Ph.D. thesis, Dept. of Civil Eng., Univ. of Tokyo, Tokyo.

Leplastrier, M., A. J. Pitman, H. Gupta, and Y. Xia (2002), Exploring the relationship between complexity and performance in a land surface model using the multicriteria method, *J. Geophys. Res.*, *107*(D20), 4443, doi:10.1029/2001JD000931.

Liang, X., D. P. Lettenmaier, E. F. Wood, and S. T. Burges (1994), A simple hydrologically based model of land surface water and energy fluxes for general circulation models, *J. Geophys. Res.*, *99*(D7), 14,415–14,428.

Liu, Y., L. A. Bastidas, H. V. Gupta, and S. Sorooshian (2003), Impacts of a parameterization deficiency on off-line and coupled land surface model simulations, *J. Hydrometeorol.*, *4*(5), 901–914.

Liu, Y., H. V. Gupta, S. Sorooshian, and L. A. Bastidas (2005), Constraining land surface and atmospheric parameters of a locally coupled model using observational data, *J. Hydrometeorol.*, in press.

Marquardt, D. W. (1983), An algorithm for least-squares estimation of nonlinear parameters, *SIAM J. Appl. Math.*, *11*, 431–441.

Mertens, J., H. Madsen, L. Feyen, D. Jacques, and J. Feyen (2004), Including prior information in the estimation of effective soil parameters in unsaturated zone modelling, *J. Hydrol.*, *294*, 251–269.

Mishra, S., and J. C. Parker (1989), Parameter estimation for coupled unsaturated flow and transport, *Water Resour. Res.*, *25*, 385–396.

Nir, A., C. Doughty, and C. F. Tsang (1992), Validation of design procedure and performance modeling of a heat and fluid transport field experiment in the unsaturated zone, *Adv. Water Resour.*, *15*, 153–166.

Pan, L., and L. Wu (1998), A hybrid global optimization method for inverse estimation of hydraulic parameters: Annealing-simplex method, *Water Resour. Res.*, *34*, 2261–2269.

Parkin, G. W., R. G. Kachanoski, D. E. Elrick, and R. G. Gibson (1995), Unsaturated hydraulic conductivity measured by time domain reflectometry under a rainfall simulator, *Water Resour. Res.*, *31*, 447–454.

Peters-Lidard, C. D., E. Blackburn, X. Liang, and E. F. Wood (1998), The effect of soil thermal conductivity parameterization on surface energy fluxes and temperatures, *J. Atmos. Sci.*, *55*, 1209–1224.

Pitman, A. J. (1994), Assessing the sensitivity of a land-surface scheme to the parameter values using a single column model, *J. Clim.*, *7*, 1856–1869.

Pitman, A. J., and A. Henderson-Sellers (1998), Recent progress and results from the project for the intercomparison of land surface parameterization schemes, *J. Hydrol.*, *212–213*, 128–135.

Pleim, J. E., and A. Xiu (1995), Development and testing of a surface flux and planetary boundary layer model for application in mesoscale models, *J. Appl. Meteorol.*, *34*, 16–32.

Sellers, P. J., W. J. Shuttleworth, J. L. Dorman, A. Dalcher, and J. M. Roberts (1989), Calibrating the simple biosphere model for Amazonian Tropical forest using field and remote sensing data. Part I: Calibration with field data, *J. Appl. Meteorol.*, *28*, 727–759.

Sellers, P. J., D. A. Randall, G. J. Collatz, J. A. Berry, C. B. Field, D. A. Dazlich, C. Zhang, G. D. Collelo, and L. Bounoua (1996), A revised land surface parameterization (SiB2) for atmospheric GCMs, Part I: Model formulation, *J. Clim.*, *9*, 676–705.

Sen, O. L., L. A. Bastidas, W. J. Shuttleworth, and Z.-L. Yang (2001), Impact of field-calibrated vegetation parameters on GCM climate simulation, *Q. J. R. Meteorol. Soc.*, *127*, 1199–1223.

Simunek, J., and M. T. van Genuchten (1996), Estimating unsaturated soil hydraulic properties from tension disc infiltrometer data by numerical inversion, *Water Resour. Res.*, *32*, 2683–2696.

Toorman, A. F., P. J. Wierenga, and R. G. Hills (1992), Parameter estimation of hydraulic properties from one-step outflow data, *Water Resour. Res.*, *28*, 3021–3028.

van de Grind, A. A., and M. Owe (1994), Bare soil surface resistance to evaporation by vapor diffusion under semiarid conditions, *Water Resour. Res.*, *30*, 181–188.

van Genuchten, M. T. (1980), A closed-form equation for predicting the hydraulic conductivity of unsaturated soils, *Soil Sci. Soc. Am. J.*, *44*, 892–898.

Yang, K., T. Koike, H. Fujii, K. Tamagawa, and N. Hirose (2002), Improvement of surface flux with a turbulence-related length, *Q. J. R. Meteorol. Soc.*, *128*, 2073–2087.

Yang, K., T. Koike, and D. Yang (2003), Surface flux parameterization in the Tibetan Plateau, *Boundary Layer Meteorol.*, *106*, 245–262.

Yang, K., T. Koike, H. Ishikawa, and Y. Mao (2004), Analysis of the surface energy budget at a site of GAME/Tibet using a single-source model, *J. Meteorol. Soc. Jpn.*, *82*, 131–153.

Yapo, P., H. V. Gupta, and S. Sorooshian (1996), Automatical calibration of conceptual rainfall-runoff models, sensitivity to calibration data, *J. Hydrol.*, *181*, 23–48.

Yapo, P., H. V. Gupta, and S. Sorooshian (1998), Multi-objective global optimization for hydrological models, *J. Hydrol.*, *204*, 83–97.

L. Bastidas, Department of Civil and Environmental Engineering and Utah Water Research Laboratory, Utah State University, Old Main Hill 4110, Logan, UT 84322-4110, USA.

T. Koike and K. Yang, Department of Civil Engineering, University of Tokyo, Hongo 7-3-1, Bunkyo-ku, Tokyo 113-8656, Japan. (yangk@hydra.t.u-tokyo.ac.jp)

B. Ye, Cold and Arid Regions Environmental and Engineering Research Institute, Chinese Academy of Sciences, 260 Donggang West Road, Lanzhou, Gansu 730000, China.